Available online at www.sciencedirect.com

SCIENCE DIRECT

Developmental Biology 286 (2005) 391 – 404

DEVELOPMENTAL BIOLOGY

www.elsevier.com/locate/ydbio

beamter/*deltaC* and the role of Notch ligands in the zebrafish somite segmentation, hindbrain neurogenesis and hypochord differentiation

Dörthe Jülich[a,1], Chiaw Hwee Lim[b,1], Jennifer Round[a], Claudia Nicolaije[a], Joshua Schroeder[a], Alexander Davies[d], Tübingen 2000 Screen Consortium[2], Robert Geisler[c], Julian Lewis[d], Yun-Jin Jiang[b,*], Scott A. Holley[a,*]

[a]*Department of Molecular, Cellular and Developmental Biology, Yale University, New Haven, CT 06520-8103, USA*
[b]*Laboratory of Developmental Signalling and Patterning, Institute of Molecular and Cell Biology, Singapore*
[c]*Max Planck-Institut für Entwicklungsbiologie, Tübingen, Germany*
[d]*Vertebrate Development Laboratory, Cancer Research UK, London, UK*

Received for publication 30 November 2004, revised 12 May 2005, accepted 17 June 2005
Available online 26 August 2005

Abstract

The Tübingen large-scale zebrafish genetic screen completed in 1996 identified a set of five genes required for orderly somite segmentation. Four of them have been molecularly identified and three were found to code for components of the Notch pathway, which are required for the coordinated oscillation of gene expression, known as the segmentation clock, in the presomitic mesoderm (PSM). Here, we show that the final member of the group, *beamter* (*bea*), codes for the Notch ligand DeltaC, and we present and characterize two new alleles, including one allele encoding for a protein truncated in the 7th EGF repeat and an allele deleting only the DSL domain which was previously shown to be necessary for ligand function. Interestingly however, when we over-express any of the mutant *deltaC* mRNAs, we observe antimorphic effects on both hindbrain neurogenesis and hypochord formation. Expression of *bea/deltaC* oscillates in the PSM, and a triple fluorescent in situ analysis of its oscillation in relation to that of other oscillating genes in the PSM reveals differences in subcellular localization of the oscillating mRNAs in individual cells in different oscillation phases. Mutations in *aei/deltaD* and *bea/deltaC* differ in the way they disrupt the oscillating expression of *her1* and *deltaC*. Furthermore, we find that the double mutants have significantly stronger defects in hypochord formation but not in somitogenesis or hindbrain neurogenesis, indicating genetically that the two *delta's* may function either semi-redundantly or distinctly, depending upon context.

Keywords: Zebrafish; Somite; Notch; After eight; DeltaD; Beamter; DeltaC; Oscillator

* Corresponding authors. Y.-J. Jiang is to be contacted at Laboratory of Developmental Signalling and Patterning, Institute of Molecular and Cell Biology, Singapore. S.A. Holley, Department of Molecular, Cellular and Developmental Biology, Yale University, P.O. Box 208103, New Haven, CT 06520-8103, USA. Fax: +1 203 432 5690.

E-mail addresses: yjjiang@imcb.a-star.edu.sg (Y.-J. Jiang), scott.holley@yale.edu (S.A. Holley).

[1] These authors contributed equally to this work.

[2] F. Van Bebber[1], E. Busch-Nentwich[1], R. Dahm[1], O. Frank[1], H.-G. Fronhöfer[1], H. Geiger[1], D. Gilmour[1], S. Holley[1], J. Hooge[1], D. Jülich[1], H. Knaut[1], F. Maderspacher[1], H.-M. Maischein[1], C. Neumann[1], C. Nüsslein-Volhard[1], H. Roehl[1], U. Schönberger[1], C. Seiler[1], S. Sidi[1], M. Sonawane[1], A. Wehner[1], P. Erker[2], H. Habeck[2], U. Hagner[2], C.E. Hennen Kaps[2], A. Kirchner[2], T. Koblizek[2], U. Langheinrich[2], C. Loeschke[2], C. Metzger[2], R. Nordin[2], J. Odenthal[2], M. Pezzuti[2], K. Schlombs[2], J. de Santana-Stamm[2], T. Trowe[2], G. Vacun[2], B. Walderich[2], A. Walker[2], C. Weiler[2]. [1]Max-Planck-Institut für Entwicklungsbiologie, Spemannstrasse 35, 72076 Tübingen, Germany; [2]Artemis Pharmaceuticals GmbH, 72076 Tübingen, Germany.

0012-1606/$ - see front matter © 2005 Elsevier Inc. All rights reserved.
doi:10.1016/j.ydbio.2005.06.040

Introduction

DeltaC is one of four known zebrafish members of the Delta subfamily of Notch ligands, all of them transmembrane proteins. Binding of a Delta family member on one cell to the transmembrane receptor Notch on another causes the intracellular domain of Notch to be proteolytically cleaved. This allows the transport of the intracellular fragment N^{ICD} to the nucleus where, in conjunction with the Suppressor of Hairless/RPB-Jκ DNA binding protein, it activates the transcription of target genes including members of the *hairy*/*enhancer of split* family, coding for bHLH transcriptional repressors (Artavanis-Tsakonas et al., 1999; Greenwald, 1998).

Experiments in mouse, zebrafish and *Xenopus* have demonstrated that Notch signaling is essential for the correct formation of somites, the segmented precursors of the vertebral column and skeletal muscle (Bessho et al., 2001; Conlon et al., 1995; del Barco Barrantes et al., 1999; Dornseifer et al., 1997; Dunwoodie et al., 2002; Evrard et al., 1998; Holley et al., 2000, 2002; Hrabé Angelis et al., 1997; Jen et al., 1997; Jen et al., 1999; Jouve et al., 2000; Kusumi et al., 1998; Oka et al., 1995; Takke and Campos-Ortega, 1999; Wong et al., 1997; Zhang and Gridley, 1998). Theories differ, however, as to the exact nature of the role that Notch signaling plays in this process (Giudicelli and Lewis, 2004). Segmentation of the paraxial mesoderm is thought to be regulated by a segmentation clock or oscillator (Cooke, 1998; Cooke and Zeeman, 1975; Meinhardt, 1982, 1986; Palmeirim et al., 1997) and (reviewed in Holley and Takeda, 2002; Pourquié, 2003; Rida et al., 2004; Weinmaster and Kintner, 2003). Somite formation is presaged by stripes of gene expression that appear within the morphologically unsegmented presomitic mesoderm (PSM). Formation of this striped prepattern depends on the segmentation oscillator that operates in the cells of the PSM, causing them to go through repeated cycles of expression and repression of genes associated with the Notch signaling pathway. The oscillation slows down towards the anterior end of the PSM, giving rise to stripes of cells in different phases, visible as spatial waves of gene expression that appear to propagate through the PSM from posterior to anterior. In the zebrafish, *deltaC* is one of the oscillating genes, and in situ hybridization with a *deltaC* probe has been used to demonstrate its oscillation and to show how it is disrupted in various mutants (Holley et al., 2002; Jiang et al., 2000). Other oscillating genes include several *hairy*/*enhancer of split*-related transcription factors in the chick, mouse and zebrafish (Bessho et al., 2001; Gajewski et al., 2003; Holley et al., 2000; Jouve et al., 2000; Leimeister et al., 2000; Oates and Ho, 2002; Palmeirim et al., 1997; Sawada et al., 2000), *lunatic fringe* (*Lfng*) in the mouse and chick (Aulehla and Johnson, 1999; Forsberg et al., 1998; McGrew et al., 1998), and *Axin2* in the mouse (Aulehla et al., 2003). In the zebrafish, these stripes travel roughly one cell diameter every 5–6 min (Holley et al., 2000). At the anterior end of the PSM, the oscillations stop and the pattern is stabilized. The moving boundary between the PSM, where oscillation occurs, and the tissue anterior to it, where oscillation is arrested and morphological segmentation begins, is called the "wave-front" (Cooke, 1998; Cooke and Zeeman, 1975).

The underlying oscillator mechanism is only beginning to be understood (reviewed in Giudicelli and Lewis, 2004). Many observations suggest that the oscillator is based on feedback loops involving the Notch signaling pathway and a number of *hairy/E(spl)*-related transcription factor genes such as *her1* and *her7* in zebrafish and *Hes7* in mouse, which are targets of the Notch pathway (Bessho et al., 2001, 2003; Gajewski et al., 2003; Hirata et al., 2004; Holley et al., 2002; Lewis, 2003; Oates and Ho, 2002). The Notch modulator Lfng is also involved in the mouse and chick (Dale et al., 2003; Serth et al., 2003). In the mouse, however, there is also evidence that a Wnt-dependent clock may act upstream of Notch (Aulehla and Johnson, 1999; Hirata et al., 2004). The wave-front that governs arrest of the oscillation and stabilization of the oscillating prepattern is thought to be specified by a gradient of Fgf signaling, which is highest in the posterior PSM (Dubrulle et al., 2001; Dubrulle and Pourquié, 2004; Sawada et al., 2001). The decline of Fgf signaling below a certain threshold defines the anterior boundary of the PSM, switching on expression of *fss*/*tbx24* (in zebrafish) as the temporal oscillation becomes arrested (Holley et al., 2000; Nikaido et al., 2002). This process results in the segmental expression of a number of genes in the somitic tissue as it emerges at the anterior end of the PSM, including *mesp* genes, Notch pathway genes and genes coding for Eph receptors and ephrins. These genes are thought to collaborate to establish the morphological somite borders via local cell signaling, cell sorting, cell polarization and extracellular matrix assembly (Barrios et al., 2003; Durbin et al., 1998, 2000; Henry et al., 2000; Hrabé Angelis et al., 1997; Jülich et al., 2005; Kim et al., 2000; Koshida et al., 2005; Kulesa and Fraser, 2002; Nakaya et al., 2004; Saga et al., 1997; Sato et al., 2002; Sawada et al., 2000; Takahashi et al., 2000; Topczewska et al., 2001).

It is one thing to show that expression of a gene oscillates, and another to show that it is an essential part of the underlying mechanism that generates oscillations. In the zebrafish, genes coding for essential components of the oscillator mechanism have been identified through a screen for mutations that disrupt the regular periodic pattern of somite segmentation, conducted as part of the large-scale genetic screens published in 1996 (Jiang et al., 1996; van Eeden et al., 1996). Five genes essential for somite segmentation were found: *fused somites* (*fss*), *after eight* (*aei*), *deadly seven* (*des*), *mind bomb* (*mib*, also known as *white tail*), and *beamter* (*bea*). Subsequent work revealed the molecular identity of four of these genes: *aei* was found to code for the Notch ligand DeltaD, *des* for Notch1a, *mib* for an E3 ubiquitin ligase that acts on Delta proteins and is

necessary to enable them to activate Notch, and *fss* for the transcription factor Tbx24 (Holley et al., 2000, 2002; Itoh et al., 2003; Nikaido et al., 2002). Further analysis demonstrated an important functional distinction: mutations in *aei*, *des*, *mib* and *bea* disrupt the coordinated oscillation of gene expression in the PSM, but mutations in *fss* do not (Holley et al., 2000, 2002; Jiang et al., 2000). This reflects the fact that *fss* comes into play only in the most anterior part of the PSM (Holley et al., 2000; Nikaido et al., 2002; van Eeden et al., 1998).

Here, we complete the cloning of the five somite segmentation genes found in the 1996 screen by identifying *bea* as the gene coding for DeltaC. Thus, all the genes in this set that are required for PSM oscillation code for Notch pathway components. To clarify the function of DeltaC and further interpret the *bea* phenotype, we compare and contrast the *bea*/*deltaC* phenotype, the *aei*/*deltaD* phenotype and the double mutant phenotype with respect to somitogenesis and two other processes, hindbrain neurogenesis and hypochord formation, that depend on Notch signaling and are disturbed in *mib*, *aei* and *des* mutant embryos (Gray et al., 2001; Holley et al., 2000; Itoh et al., 2003; Jiang et al., 1996; Latimer et al., 2002). Through detailed examination of the in situ hybridization patterns of *deltaC* and *her1* that reveal the changing subcellular localization of the mRNAs at different stages of the somitic oscillation cycle, we show how the relative expression of these genes is affected in *aei* and *bea* mutants. This analysis indicates that *deltaC* and *deltaD* have similar, parallel functions in some processes, but that in somitogenesis they have largely distinct roles that are both necessary for the coordinated oscillation of gene expression in the cells of the PSM.

Materials and methods

Embryos

Wild-type, *beamter* (*bea*^{tw212b}, *bea*^{tm98}, *bea*^{to202}, *bea*^{tit446}, *bea*^{thf102}) and *after eight* (*aei*^{tr233}, *aei*^{tg249}) mutant embryos (van Eeden et al., 1996) were raised as previously described (Kimmel et al., 1995). *bea*^{tit446}, *bea*^{thf102} are new alleles of *beamter* found in the Tübingen 2000 genetic screen.

Mapping and sequencing

Meiotic mapping of *bea* was performed essentially as described (Nüsslein-Volhard and Dahm, 2002). Allele sequence was determined by sequencing at least two RT-PCR products for each *bea* allele.

RNA synthesis and injections

Capped mRNAs were synthesized using the mMessage mMachine kit (Ambion). For each different construct, 3.5–4.0 nl mRNA at concentration of approximately 11 ng/μl was injected into the yolks of 1- to 4-cell stage embryos.

Whole-mount mRNA in situ hybridization

Digoxigenin-labeled RNA antisense probes were generated with a Stratagene RNA transcription kit. Single whole-mount in situ hybridizations were done as previously described (Oxtoby and Jowett, 1993).

Double fluorescent in situ hybridization

Digoxigenin and fluorescein-labeled probes were made via standard protocols. The in situ protocol was adapted from previous protocols (Hammerschmidt and Nüsslein-Volhard, 1993; Jowett, 2001). For the protocol to work as presented, all probes, reagents and POD substrates must be optimal.

Fixation

Embryos were fixed with 4% PFA/PBS overnight at 4°C, washed 2 × 5 min in PBS, 5 min at room temperature (RT), manually dechorionated and then transferred to 25%, 50% and 75% methanol (MeOH) for 5 min each. Embryos were then placed in 100% (MeOH) which was replaced with fresh methanol after 5 min and dehydrated overnight (ON) at −20°C. Embryos were then brought through 75%, 50%, and 25% MeOH for 5 min each at RT and then twice for 5 min in PBST. Embryos were then fixed for 20 min in 4% PFA at RT and wash 2 × 5 min in PBST.

Proteinase treatment

Embryos were digested with proteinase K (5 mg/ml in PBST) at RT for 5 min. Embryos were quickly washed 2× in PBST and fixed in 4% PFA for 20 min. Embryos were washed 2 × 5 min in PBST.

Prehybridization and hybridization

Embryos were incubated 5 min at 55°C in HYB− (50% formamide, 5× SSC and 0.1% Tween-20). The embryos were then changed to HYB+ (HYB−, 5 mg/ml torula (yeast) RNA, 50 μg/ml heparin) and were incubated for at least 1 h at 55°C. Probe was added to the embryos and incubated overnight at 55°C. From this point forward, the tubes were covered in aluminum foil. Probe was removed, and embryos washed in 50% formamide/2× SSC twice for 30 min, washed in 2× SSC for 15 min, and washed in 0.2× SSC for 30 min. All washes at 55°C.

Detection of fluorescein-labeled probe

Embryos were blocked for at least 60 min at RT with 150 mM maleic acid, 100 mM NaCl (pH 7.5) plus blocking reagent (2% Roche Blocking Reagent). Anti-FL POD (Roche) was added at a 1:500 dilution in above solution and embryos were incubated at 4°C ON. Embryos were washed 4 × 20 min in 1× maleic acid buffer and 2 × 5 min in PBS all at RT. Embryos were incubated for 45 min in TSA

Plus Fluorescein Solution (Perkin Elmer) (the fluorescein-tyramide substrate was centrifuged briefly before making staining solution and then diluted 1:50 in amplification buffer). Embryos were washed 10 min each in 30%, 50%, 75% and 100% methanol in PBS. To inactivate the POD, embryos were incubated in 1% H_2O_2 in 100% methanol for 30 min at RT. Embryos were then washed 10 min each in 75%, 50% and 30% methanol in PBS and then 2 × 10 min in PBS.

Detection of digoxygenin-labeled probe

Embryos were blocked for at least 1 h at RT as above. Then, the anti-DIG POD antibody (Roche) was added at a 1:1000 dilution in block solution and the embryos incubated at 4°C ON. Embryos were then washed and stained as above with the Cy3-tyramide substrate (Perkin Elmer). After staining the embryos were washed 6 × 10′ in PBST.

β-catenin detection

Embryos were blocked for 60 min at RT in 2% Roche Blocking Reagent. The anti-β-catenin antibody (rabbit polyclonal) was added 1:100 in blocking reagent and incubated at 4°C ON. Embryos were washed 5 × 30 min in PBST, fixed for 20 min in 4% PFA and washed 2 × 5 min in PBST. Embryos were blocked for 60 min in 2% Roche Blocking Reagent and then an anti-rabbit-Alexa647 antibody was added (1:500). Embryos were incubated ON at 4°C, washed 12 × 5 min in PBST and then transferred, incubated 10 min each in 25% and 50% glycerol in PBST. The embryos were then incubated ON in 75% glycerol to make them more amenable to subsequent dissection.

Results

bea mutants show neurogenic and midline phenotypes

bea mutant embryos have somite phenotype similar to that seen in *aei*, *des* and *mib* embryos (van Eeden et al., 1996). Furthermore, the latter three also show a neurogenic phenotype, an indication of failure in Notch activation (Jiang et al., 1996; Holley et al., 2000; Gray et al., 2001). We suspected that *bea* mutation also lies in the Notch pathway as the somite studies suggest. To test this hypothesis, *huC*, a pan-neuronal marker (Kim et al., 1996), was used to check whether *bea* mutants have the suspected neurogenic phenotype in the hindbrain region due to a failure of lateral inhibition. In wild-type embryos, *huC* is segmentally and bilaterally expressed in each rhombomere, with two anterior and two posterior clusters (Fig. 1A). *aei* mutants showed a neuronal hyperplasia, affecting a broader class of cells (Figs. 1B, C). Similarly, in *bea* mutants, *huC* expression became locally up-regulated and, in some cases, the anterior and posterior clusters were fused (Figs. 1D–H).

It has been shown that both *deltaC* and *deltaD* are required for hypochord cells differentiating from midline precursors (Latimer et al., 2002). To test whether the hypochord is affected in *bea* mutants, we examined *col2a1* expression (Yan et al., 1995). Similar to *aei* mutants (Fig. 1L), all *bea* mutants exhibit a hypochord phenotype, ranging from gaps within hypochord cells (Figs. 1M–N) to elongated but fewer hypochord cells (Figs. 1O–P).

beamter is deltaC

The results shown above suggest that *bea* works closely with Notch signaling. But could it be *deltaC*? *bea* was mapped to linkage group (LG) 15, 4 cM from z8991 (125 recombinations in 3138 meioses) and 0.2 cM from z7871 (4 recombinations in 2032 meioses) (Fig. 2A). Concurrently, we mapped *deltaC* to the same cluster as z7871 by radiation hybrid mapping (Geisler et al., 1999; Smithers et al., 2000). The fact that *bea* and *deltaC* mapped so closely to each other on LG15, along with the observed similarities between the *bea* mutant phenotype and the *deltaC* morphant, suggested that *bea* codes for DeltaC (Holley et al., 2002; Oates et al., 2005). Thus, we examined the coding sequence of *deltaC* in each of five *bea* alleles (Fig. 2B). Alleles bea^{thf102} and bea^{tit446}, isolated in the Tübingen 2000 screen, contained the most severe alterations in the *deltaC* coding sequence. bea^{thf102} contains a deletion that is predicted to remove amino acids 143 to 201 and replace them with a single alanine residue. This deletion eliminates the DSL domain which is required for ligand function (Fitzgerald and Greenwald, 1995; Henderson et al., 1997). bea^{tit446} contains a premature stop codon within the 7th EGF repeat, producing what should be a functionally null allele. Analysis of the Tübingen 1996 alleles revealed mutations also producing amino acid substitutions within the extracellular domain of DeltaC (see Fig. 2B). Homozygotes of each allele give rise to fertile adults. Together, the mapping and sequence data indicate that the *bea* mutant phenotype is caused by mutation in *deltaC*.

The loss of hypochord cells in different mutants can be easily quantified and provides an objective way to compare the strength of the different *bea* alleles. In terms of genetic severity in hypochord: *tit446* ≈ *to202* > *tm98* > *tw212b* ≈ *thf102* (Figs. 1M–P and legend). While *tit446* is probably a null allele, *thf102* behaves as a likely hypomorphic allele. This is notable in that the *thf102* allele is a fairly precise deletion of the DSL domain, implying that DeltaC retains some ability to activate Notch even when its DSL domain is missing. The three missense alleles *to202*, *tm98* and *tw212b* containing amino acid substitutions in different EGF repeats (Fig. 2B) display null to hypomorphic phenotypes.

Injection of mutant deltaC mRNA phenocopies bea phenotypes

To further characterize the different *bea*/*deltaC* alleles, we overexpressed the mutant mRNAs via injection of synthetic transcripts and assayed their effects on morphol-

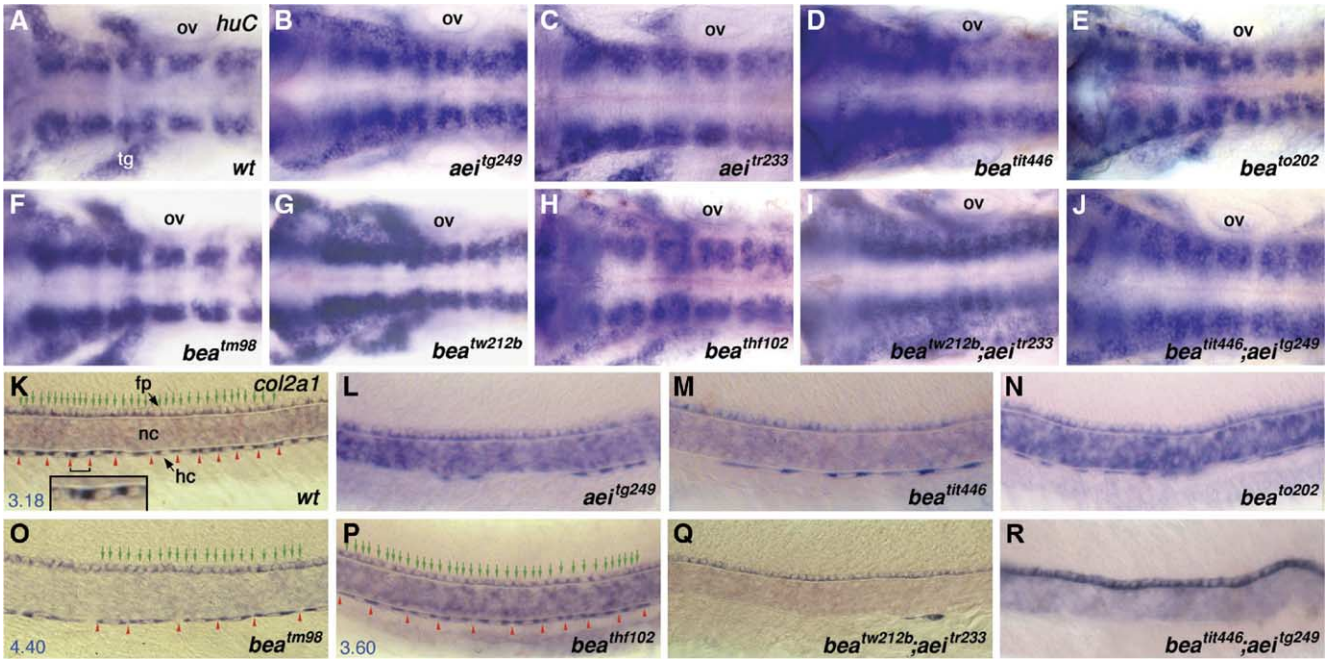

Fig. 1. Molecular phenotypes of *bea*, *aei* single and *bea*/*aei* double mutants during neurogenesis and hypochord formation. In situ hybridization of *huC* at approximately 30 hpf (A–J). Embryos of wild-type (A), aei^{tg249} (B), aei^{tr233} (C), bea^{tit446} (D), bea^{to202} (E), bea^{tm98} (F), bea^{tw212b} (G), bea^{thf102} (H), bea^{tw212b}; aei^{tr233} (I) and bea^{tit446}; aei^{tg249} (J). Note that the hindbrain neurons are increased in *bea* and *aei* single mutants as well as in *bea*/*aei* double mutants. Otic vesicle (ov) is the landmark for rhombomere 5. Lateral views of embryos labeled for *col2a1* RNA expression at approximately 30 hpf (K–R). In wild-type embryo (K, fp/hc = 3.04 ± 0.32, $n = 6$), *col2a1* is expressed in floor-plate (fp) cells and hypochord (hc) cells, immediately dorsal to and ventral to notochord (nc), respectively. Bracket denotes one hypochord cell, whose enlargement is shown in the insert. Each green arrow indicates a floor-plate cell; each red arrowhead indicates the boundary between two hypochord cells. The blue number at the bottom left corner is the number ratio of floor-plate cells to hypochord cells (fp/hc). Obvious gaps in hypochord can be seen in aei^{tg249} (L), bea^{tit446} (M), bea^{to202} (N) and bea^{tw212b}; aei^{tr233} (Q) mutants, indicating a reduction in the numbers of differentiated hypochord cells while putative double null bea^{tit446}; aei^{tg249} (R, $n = 5$) have no hypochord cells. Though there is no obvious gap, hypochord cells in bea^{tm98} (O, fp/hc = 4.56 ± 0.47, $n = 6$) and bea^{thf102} (P, fp/hc = 3.36 ± 0.17, $n = 3$) mutants are elongated and, therefore, reduced in number and increased in fp/hc ratio (compare the fp/hc ratio and/or the length of hypochord cell to that of wild-type embryos). All floor plate cells look normal. Anterior is to the left (A–R) and dorsal to the top (K–R). Abbreviation: fp, floor plate; hc, hypochord; nc, notochord; ov, otic vesicle; tg, trigeminal ganglion neurons. fp/hc ratio is expressed in average ± standard deviation format; *n*: numbers of examined embryos.

ogy, hindbrain neurogenesis and hypochord formation. Two *bea* mutations, bea^{tm98} (T443P, ACC → CCC) and bea^{tw212b} (C446S, TGC → AGC), are located in the seventh EGF repeat of DeltaC. Six cysteine residues are conserved in all EGF repeats of Delta and Notch proteins. Thus, the substitution of cysteine with serine in position 446 is likely to be responsible for the bea^{tw212b} phenotype. Indeed, two *Drosophila Delta* mutations affecting such conserved cysteines, Dl^{BE21} (C301S) and Dl^{CE9} (C301Y), and one similar zebrafish *deltaA* mutation, $deltaA^{dx2}$ (C308Y) (in the second EGF repeat), have been demonstrated to be responsible for the corresponding phenotypes (Appel et al., 1999; Parks et al., 2000). It is not certain that the substitution of tyrosine with proline in position 443 found in bea^{tm98} is responsible for the mutant phenotype. However, it seems probable, since this residue is part of a tetrapeptide (443–446, in DeltaC numbering) which is relatively conserved in the seventh EGF repeat in a subset of Delta proteins: DeltaC (TCTC), DeltaB (TCTC), DeltaD (TCTC), X-Delta-1 (SCTC), X-Delta-2 (TCSC), C-Delta-1 (SCTC), human DLL1 (SCTC), rat Dll1 (SCTC) and mouse Dll1 (SCTC).

We injected the corresponding *deltaC* mRNA ($deltaC^{C429X} = bea^{tit446}$; $deltaC^{T443P} = bea^{tm98}$; $deltaC^{C446S} = bea^{tw212b}$) and a doubly mutant mRNA ($deltaC^{T443P,\ C446S}$) into wild-type embryos and studied the hindbrain neuron and hypochord phenotypes. The segmentation phenotype was not analyzed, since both wild-type and dominant-negative Delta constructs can lead to similar somite abnormalities (Jen et al., 1997; Takke and Campos-Ortega, 1999). While the injection of wild-type *deltaC* mRNA resulted in a reduction of neurons demonstrated by *huC* expression (compare Figs. 3G to F), the injection of the other three constructs caused a neuronal hyperplasia (Figs. 3H–J). Likewise, in embryos stained for *col2a1* expression to show the hypochord phenotype, the injection of mutant *deltaC* mRNA phenocopied *bea* mutants, with reduced numbers of hypochord cells (Figs. 3M–P), whereas injection of wild-type *deltaC* mRNA had an opposite effect (Fig. 3L). The penetrance of the neuronal phenotype due to mRNA injection is high, but that of the hypochord phenotype is low, probably because of the small size of the midline precursor domain (Latimer et al., 2002). The effects of injection of the doubly-mutant mRNA were

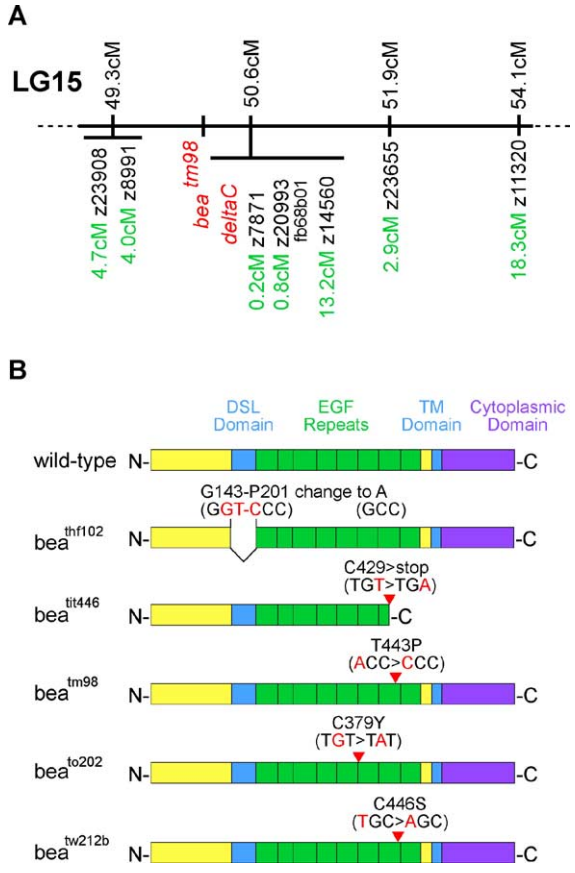

Fig. 2. *beamter* encodes *deltaC*. (A) The region of linkage group 15 to which *bea* and *deltaC* were mapped. *bea* was mapped via meiotic recombination relative to simple sequence repeat polymorphisms (SSLPs) being placed 0.2 cm from z7871. The map distances in the public database are in black while our map distances between *bea* and the SSLPs are indicated in green. Discrepancies between our map and the public database likely reflect differences in the number of meioses used for mapping. Most of the SSLPs were originally mapped using 96 meioses. We used 528 meioses to map *bea* relative to z23908, 3138 for z8991, 2032 for z7871, 122 for z20993, 804 for z14560, 804 for z23655 and 2704 for z11320. Radiation hybrid mapping placed *deltaC* in the same cluster as z7871, z20993, the EST fb68b01 and z14560. (B) The coding sequence from each *beamter* allele was determined by sequencing at least 2 independent RT-PCR products from each allele. The amino acid sequence refers to the published *deltaC* sequence. bea^{thf102} contains an in-frame deletion that removes DSL domain. bea^{tit446} contains a premature stop codon in the 7th EGF repeat. These two alleles were isolated in the Tübingen 2000 Zebrafish Screen. Examination of the alleles from the Tübingen 1996 screen identified four missense mutations in bea^{to202}, bea^{tm98} and bea^{tw212b} alleles, three of which are found in each allele, including bea^{thf102} and bea^{tit446}, and thus represent polymorphisms between the Tübingen strain and the strain used to generate the published *deltaC* sequence (Smithers et al., 2000). The polymorphisms are S133G (AGT → GGT), R144E (CGA → GAG) and SP564.565ST (TCACCT → TCCACT). The remaining substitutions, each unique to the bea^{to202}, bea^{tm98} and bea^{tw212b} alleles are the likely cause of the *bea* mutant phenotype in each allele.

similar to those of injection of the singly-mutant forms, but more extreme (compare Figs. 3H to I–J for neurogenesis and Figs. 3N to O–P for hypochord). The antimorphic effect of the T443P and C446S mutant mRNAs confirms that these mutations are responsible for bea^{tm98} and bea^{tw212b} phenotypes, respectively, and that the integrity of the 7th EGF repeat is required for Delta-dependent Notch activation.

Surprisingly, injection of mRNAs encoding the more severe alleles that either delete the DSL domain (thf102) or have a premature stop codon C429X (tit446), also display antimorphic activity (Figs. 3E and M). Since the mutations when inherited in the normal fashion are nevertheless recessive, this perhaps suggests that at wild-type expression levels, the mutant alleles result in a loss-of-function phenotype due to a inability to activate Notch and have little or no antimorphic effects. Conversely, when the mutant proteins are over-expressed via mRNA injection, they either bind to Notch but fail to trigger its activation or interfere with other cellular machinery necessary for transduction of a Notch signal.

Double fluorescent in situ analysis of the somite clock in wild-type, bea and aei embryos reveals differences in the deltaC oscillation relative to that of her1

To clarify the role of *bea/deltaC* in the prepatterning of the somitic mesoderm, we developed a double fluorescent in situ protocol that vastly improves the ability to examine overlapping gene expression patterns and provides sub-cellular resolution of mRNA distribution. We used tyramide-fluorescein to visualize *her1* mRNA (Figs. 4A, D), tyramide-Cy3 to visualize *deltaC* mRNA (Figs. 4B, D) and an Alexa647 secondary antibody to visualize β-catenin, whose cortical distribution outlines the cell (Figs. 4C, D). Using this protocol, one can observe the different cell states corresponding to different phases of oscillation within each stripe of gene expression. In the anterior of each stripe, one often can see small, intense spots of gene expression (labeled 1 in Figs. 4E–G). In the middle of the stripe, defined regions of mRNA localization are observed (labeled 2 in Figs. 4E–G), while in the posterior of the stripes, the mRNAs appear throughout the cell (labeled 3 in Figs. 4E–G). We interpret these subregions of each stripe of gene expression as representing (1) transcription at the chromosomal loci, (2) pan-nuclear distribution of the transcript and (3) broad cytoplasmic distribution of the transcript with little or no active transcription of the oscillating genes.

The evidence that pattern (1) represents transcription at individual chromosomal loci is supported by several observations. First, these spots are confined to the anterior of each stripe of oscillating gene expression and thus are not non-specific background. When *her1* expression is visualized along with nuclear visualization via propidium idodide staining (Fig. 4G), the spots of gene expression are clearly nuclear. Additionally, only one or two spots are typically seen for each gene per nucleus (Figs. 4D–J). When *deltaC* and *her1* are visualized in the same cells, the intense spots do not overlap (Fig. 4E), which is expected since the two genes are on separate chromosomes. By contrast, *her1* and *her7* are on the same chromosome,

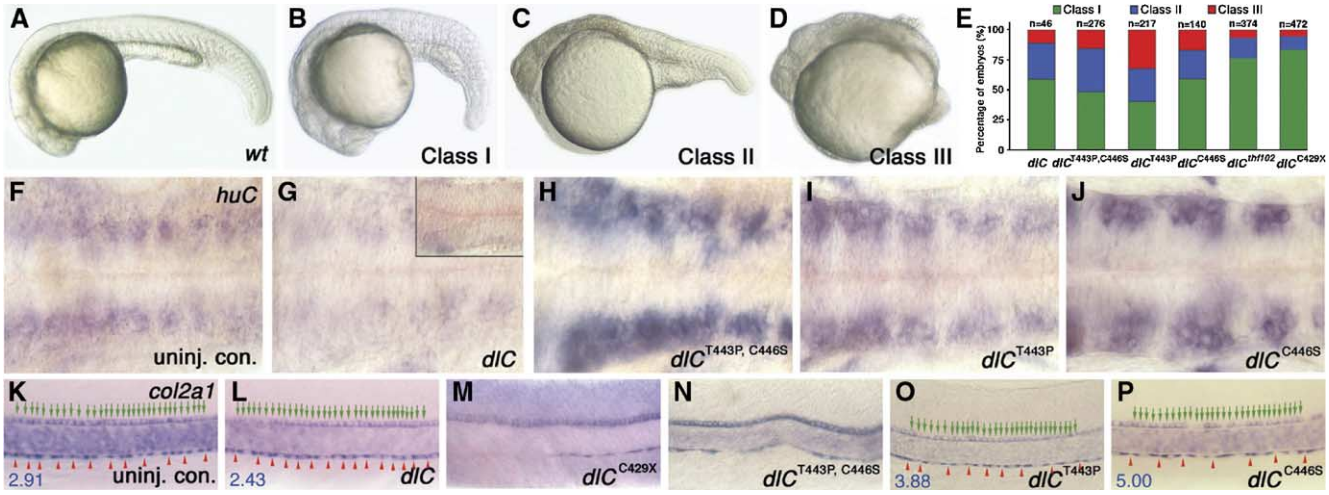

Fig. 3. Morphology and molecular characterization of embryos injected with different constructs of *deltaC* mRNA. (B–D) Injected embryos display a range of phenotypes that can be grouped into three distinct classes showing various degrees of retarded growth and axial defects. Wild-type (A, wt) at approximately at 22 hfp, Class I (B) embryo with delayed growth, Class II (C) embryo with retarded growth, malformed tail and short body axis and Class III (D) embryo with severe retarded growth, short body axis without notochord and somites (with defects mainly attributed to injection artifacts). (E) Bar graph displays the relative proportions of each morphological class in response to the different constructs of *deltaC* mRNA injected, *n*: numbers of examined embryos. *huC* staining of uninjected control (F), class I *dlC*-injected (G, class II in the insert), class I $dlC^{T443P,\ C446S}$-injected (H), class I dlC^{T443P}-injected (I) and class I dlC^{C446S}-injected (J) embryos at approximately 30 hpf. Note that while neurons are increased in $dlC^{T443P,\ C446S}$-, dlC^{T443P}- and dlC^{C446S}-injected embryos, *huC*-positive neurons are decreased in *dlC*-injected embryos. Lateral view of ~30 hpf embryos labeled for *col2a1* RNA expression in uninjected control (K, fp/hc = 3.04 ± 0.32, *n* = 6), class I *dlC*-injection (L, fp/hc = 2.32 ± 0.10, *n* = 5), class I dlC^{C429X}-injection (M): 30.4% (52/171) embryos have more severe anterior hypochord phenotype than uninjected bea^{tit446} mutants; 75% (42/56) class II dlC^{C429X}-injected embryos have more severe anterior hypochord phenotype, class I $dlC^{T443P,\ C446S}$-injection (N): 11.5% (7/61) embryos have gaps in between hypochord cells while 88.5% embryos (54/61) have small and localized gaps (not shown), class I dlC^{T443P}-injection (O): most of the embryos were found to have floor-plate and hypochord cells morphologically similar to those of bea^{tm98} mutant, while 6.9% (3/43) of the embryos have gaps in hypochord (not shown) and class I dlC^{C446S}-injection (P): 57.1% (12/21) embryos have elongated hypochord cells. Each green arrow indicates a floor-plate cell; each red arrowhead indicates the boundary between two hypochord cells. The blue number at the bottom left corner is the ratio of number of floor-plate cells to number of hypochord cells (fp/hc). All floor cells plate look normal. Anterior is to the left (F–O) and dorsal to the top (K–O). fp/hc ratio is expressed in average ± standard deviation format; *n*: numbers of examined embryos.

separated by only 12 kb (Gajewski et al., 2003; Henry et al., 2002) and when the expression of these two genes are examined in the same cells, the intense spots of each transcript co-localize (Figs. 4H–J).

The evidence that patterns (2) and (3) represent pan-nuclear and broad cellular distribution is also supported by co-staining of *her1* expression with propidium idodide. Pattern (2) in Figs. 4F–G shows that the mRNA localization is pan-nuclear. Interestingly, in the posterior of a stripe of gene expression, a cell with exclusively cytoplasmic localization of *her1* mRNA can be seen (arrow in Figs. 4F–G). This cell has stopped transcribing *her1*, exported the mRNA from the nucleus, is degrading the cytoplasmic mRNA and in 5–10 min would be completely devoid of detectable transcript.

The visualization of different phases of the oscillations in the double fluorescent in situ hybridization is also informative in considering the regulation of the different oscillating genes. Comparison of *her1* and *deltaC* expression in staged, fixed embryos indicates that (A) in the middle stripe in the PSM *deltaC* expression generally precedes *her1* expression and (B) *deltaC* expression switches from anterior half somite to posterior half somite during border morphogenesis. Embryos were fixed at the 10-somite stage, processed for in situ hybridization and then staged according to the distances between the stripes of gene expression and the morphological somite borders. Three embryos of increasing age are shown in Fig. 5.

As has been noted previously, initiation of *deltaC* transcription can precede initiation of *her1* transcription (Oates and Ho, 2002). However, we consistently observe this in only the middle stripe in embryos with three stripes of oscillating gene expression (Figs. 4D, E and Figs. 5A–C). Examination of this expression in carefully staged embryos indicates that at least *some* of the *deltaC* expressing cells in the middle stripe will ultimately express *her1* as well. However, the natural variation in somite size precludes us from determining if *all* of the *deltaC* expressing cells will express *her1* by comparing distances between the expression domains and the morphological borders. Notably, in the stripes anterior and posterior to the middle stripe, *her1* and *deltaC* show a more coincident initiation of transcription. Further, even in the middle stripe, *her1* expression precedes *deltaC* expression in some cells (Fig. 4E). Whether this local variation is simply noise within the oscillator or indicative of specific regulatory interactions is unclear at this time. However, the fact that this middle stripe generally shows *deltaC* expression prior to *her1* expression is suggestive of changes to the oscillator circuit in this region of the PSM. In this regard, it is important to

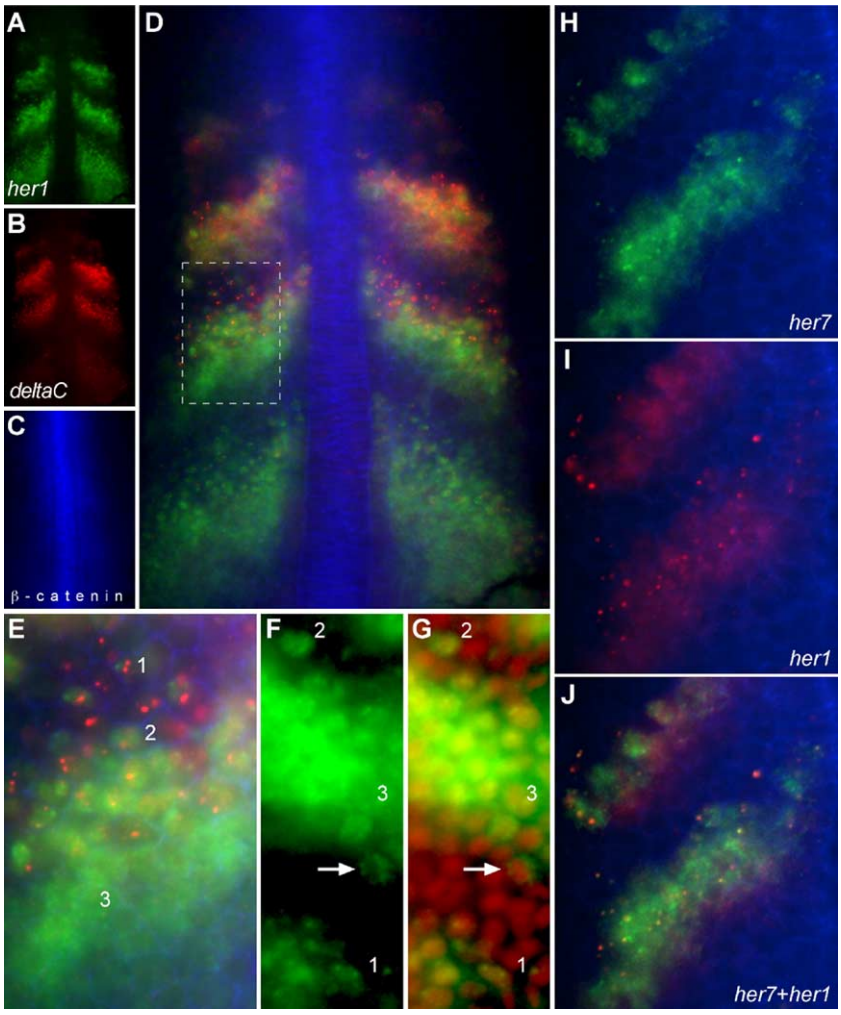

Fig. 4. Single-cell resolution of distinct phases of oscillations in transcription within the PSM. (A–E) A wild-type embryo stained for *her1* mRNA (A), *deltaC* mRNA (B) and β-catenin protein (C). β-catenin protein in the cell cortex outlines each cell, allowing the examination of cell morphology and gene expression in the same cells. (D) Overlay of A, B and C. (E) Higher magnification view of the boxed region in D. In D, one can see that *her1* and *deltaC* are differently regulated and that generally *deltaC* expression precedes (is shifted anteriorly relative to) *her1* expression in the middle stripe, but not the other two stripes. However, in E, cells within the anterior of the middle stripe that express *her1* but not yet *deltaC* can be seen. Note that *her1* expression is more intense than *deltaC* expression in the posterior stripe and less intense than *deltaC* expression in the most anterior stripe, so that the "center of gravity" of the *her1* distribution as a whole is posterior to that of the *deltaC* distribution. Also in E, three general patterns of mRNA localization can be seen. Pattern 1 appears as one or two intense spots while pattern 2 is broader but still restricted. In pattern 3, the mRNA is localized throughout the cell. Note that the intense spots of *her1* and *deltaC* do not co-localize. (F, G) Patterns 1 and 2 are restricted to the nuclei. *her1* mRNA localization (F) is compared to nuclei (red, propidium idodide staining) (G). The intense spots of pattern 1 co-localize to the nucleus suggesting that they may represent nascent transcripts at the *her1* genomic loci. Pattern 2 co-localizes with the nucleus. The arrow shows a cell within the posterior of a stripe no longer is transcribing *her1* and has exported most of the *her1* mRNA into the cytoplasm. (H–J) Show the co-localization of the intense, subnuclear spots of *her7* expression (H, green) and *her1* expression (I, red). β-catenin localization is in blue in all panels. (J) Overlay of H and I. Since *her1* and *her7* are on the same chromosome, separated by only 12 kb, one would expect the intense, nuclear spots to co-localize if those spots represent nascent transcripts at the chromosomal loci. Likewise, the pattern 1 spots of *deltaC* and *her1* would not be expected to co-localize since the two genes are on different chromosomes. (A–E, H–J) are wide-field images. (F, G) are confocal images. All panels are dorsal views of dissected tailbuds with anterior up.

note that the offsetting of the *deltaC* stripe relative to *her1* occurs even in the absence of *fss*/*tbx24* function (not shown).

In the anterior PSM, *her1* and *deltaC* expression mark the anterior half-somite. As morphological border formation proceeds, *her1* expression disappears while *deltaC* expression begins to straddle the border. As somitogenesis continues, *deltaC* expression will be confined to the posterior of each somite. In Fig. 5A, a full somite length, roughly 4–5 cells, separates the stripe of *her1*/*deltaC* in the anterior PSM from the *deltaC* stripe in the posterior of the most recently formed somite, SI. In Fig. 5B, a slightly older embryo where a new somite border is forming, shows a fading *her1* stripe flanking the posterior of the border separating S0 and SI. Meanwhile, the *deltaC* stripe straddles the forming border. In Fig. 5C, the oldest embryo displays *deltaC* expression to the anterior of the most recently formed border (in the posterior of SI) while some lateral

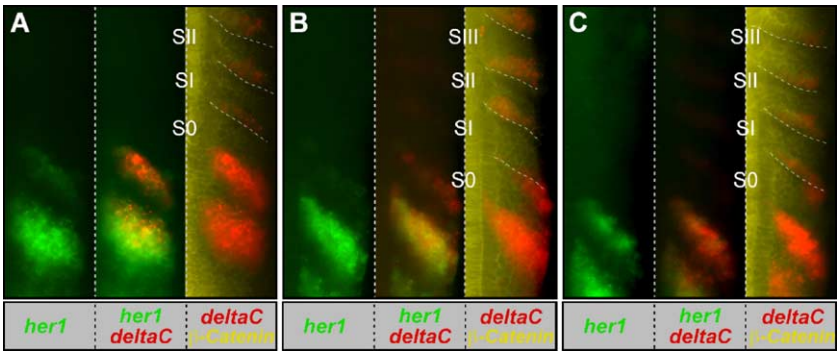

Fig. 5. Analysis of *her1* and *deltaC* expression in staged embryos reveals *deltaC* expression in transition from anterior half-somite to posterior half-somite. (A–C) shows the right half of the trunk of three progressively older embryos. These embryos were fixed at the 10 somite stage, processed to visualize *her1* mRNA (green), *deltaC* mRNA (red) and β-catenin protein (yellow). The embryos were more precisely staged by measuring the distances between the expression domains and the morphological somite borders. Embryos with decreasing distances between the expression domains and borders are considered progressively older (Holley et al., 2000). For each embryo, *her1* expression is shown alone (left) or overlain with *deltaC* expression (middle). *deltaC* expression is also overlain with β-catenin localization (right). Note that since the somitic expression of *deltaC* is weak relative to the PSM expression, in the *deltaC*/β-catenin overlay, we have altered the levels of the only somitic expression in order to visualize this expression without saturating the PSM expression. The somite borders are highlighted (dashed lines).

expression persists posterior to the border in S0. In each of the embryos shown in Fig. 5, the more mature somites, SII and SIII, exhibit *deltaC* expression in the posterior.

We further examined the relative expression patterns of *her1* and *deltaC* in embryos mutant for either of the two *delta* genes (Figs. 6A–F). In both mutants, *her1* and *deltaC* show a salt-and-pepper pattern of expression in the anterior PSM. In *aei* mutants, the domains of the two genes overlap more or less precisely. In *bea* embryos, by contrast, the *her1* domain appears slightly but significantly shifted posteriorly relative to the *deltaC* domain, and extends down into the middle part of the PSM. Comparison with the wild-type shown in Fig. 4D suggests that the *bea* pattern reflects the delay that is normally seen between peak expression of *deltaC* and peak expression of *her1*. Loss of *aei*/*deltaD*, however, appears to reduce or eliminate this *her1-deltaC* delay.

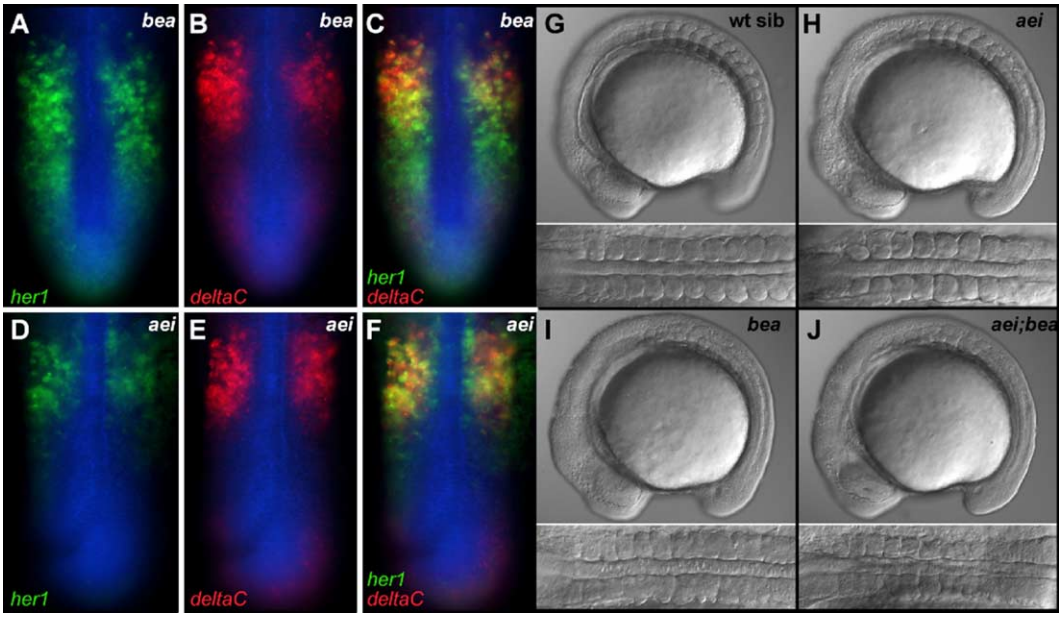

Fig. 6. The oscillating expression patterns of *her1* and *deltaC* are differentially affected in *bea*/*deltaC* and *aei*/*deltaD* mutants. (A–C) Show a *bea*/*deltaC*^{tit446} embryo stained for *her1* mRNA (A, green), *deltaC* mRNA (B, red) and β-catenin protein (blue). (C) Overlay of A and B. The "salt and pepper" pattern of *her1* extends more posteriorly than that of *deltaC*. (D–F) Show an *aei*/*deltaD*^{tg249} embryo stained for *her1* mRNA (D, green), *deltaC* mRNA (E, red) and β-catenin protein (blue). (F) Overlay of D and E. The "salt and pepper" patterns of *her1* and *deltaC* are both restricted to the anterior PSM. (G–J) Lateral and dorsal views of wild-type (G), *aei*/*deltaD*^{tg249} homozygotes (H), *bea*/*deltaC*^{tit446} homozygotes (I) and *aei*/*deltaD*^{tg249}; *bea*/*deltaC*^{tit446} double homozygotes (J). At the 11 somite stage, there is no clear difference in the somite phenotype when comparing the *bea*/*deltaC* homozygotes to *aei*/*deltaD*; *bea*/*deltaC* double homozygotes.

bea/deltaC and aei/deltaD have non-overlapping and overlapping functions in hindbrain neurogenesis and hypochord formation, respectively

What are the functions of *deltaC* and *deltaD* in different tissues? We first examine hindbrain neurogenesis and hypochord formation. The *bea*; *aei* double mutants (Figs. 1I, J), particularly the putative double null (*bea*^{tit446}; *aei*^{tg249}), did not have a dramatically-increased *huC* expression relative to single mutants, but showed a phenotype consistent with occurrence of neuronal hyperplasia in both the groups of neurons affected in the single mutants. This suggests that *deltaC* and *deltaD* do not have overlapping functions in hindbrain neuron development, but are responsible for lateral inhibition in distinct sets of cells, in accordance with their distinct and largely non-overlapping expression patterns in the early CNS.

In contrast, *deltaC* and *deltaD* have an overlapping function in the hypochord: a comparable but more extreme phenotype, with very few hypochord cells, developed in *bea*; *aei* double homozygotes (Figs. 1Q, R), consistent with the published finding that *deltaC* and *deltaD* have quasi-redundant functions – that is, both act in a similar way, contributing to the same effect – in hypochord development (Latimer et al., 2002).

bea/aei double mutant embryos show the same onset of the somite phenotype as bea mutant embryos

bea/*deltaC* embryos show an earlier onset of aberrant somitogenesis than *aei*/*deltaD* embryos (Figs. 6H, I) (Jiang et al., 2000; van Eeden et al., 1996, 1998). Additionally, *deltaC* expression oscillates in the posterior PSM, but *deltaD* expression does not oscillate, and, as shown above, *bea/deltaC* and *aei/deltaD* mutants display distinct effects on oscillating gene expression in the anterior PSM (Holley et al., 2002). This suggests that the two genes have distinct functions in somitogenesis. To examine this genetically, we created double mutant embryos harboring putative null mutations in both *bea*/*deltaC* and *aei*/*deltaD*. However, crosses of *bea*^{tit446}/+; *aei*^{tg249}/+ doubly heterozygous fish produced no distinct class of embryos that could be identified as having a somitogenesis defect markedly more severe than, or different from, that seen in simple *bea* homozygotes (Figs. 6I, J). This is consistent with a previous report that *bea/bea;aei/aei* double homozygotes have a somite phenotype no more severe than that of *bea/bea* simple homozygotes (van Eeden et al., 1998). When we raised to adulthood the most severely affected embryos from a cross of bea/+; *aei*/+ parents and genotyped them via complementation analysis, we found that two were *bea*/*bea*; *aei*/*aei* but seven were *bea*/*bea*; *aei*/+. This indicates that we were not able to phenotypically distinguish the double homozygotes, but also shows that double homozygotes are viable and fertile. A reservation is that we may have enriched for double homozygotes when we initially sorted the embryos by phenotype prior to rearing, but that a disproportionate number of the double homozygotes died prior to adulthood.

While the analysis of the double homozygotes unequivocally indicates that *aei* is not responsible for the formation of the anterior somites in *bea* homozygotes, we noticed that some *bea*/+;*aei*/*aei* embryos had an onset of the segmentation defect around the 3rd–5th somite suggesting that partial loss of *bea* signaling can enhance the *aei*/*deltaD* phenotype. This implies that *bea* may partially substitute for loss of *aei*. However, the preponderance of evidence indicates that *aei*/*deltaD* and *bea*/*deltaC* have largely distinct functions in establishing the segmented, somitic pattern.

Discussion

The zebrafish somite-segmentation mutants: notch but no her's, fgf's or wnt's?

The great advantage of forward genetics is that it identifies genes necessary for a given process without bias with regard to their molecular identity. Given that the somites are such an obvious feature of the zebrafish embryo, mutations affecting the placement of somite boundaries were easily identified, with an average of 4 alleles for each known member of this class of somite-segmentation genes compared with an average of 2.4 alleles per gene for the Tübingen 1996 screen as a whole (Haffter et al., 1996; van Eeden et al., 1996). With the identification of *bea*/*deltaC*, all of these somite-segmentation genes have been cloned and 4 of the 5 code for components of the Notch pathway (Holley et al., 2000, 2002; Itoh et al., 2003; Nikaido et al., 2002). This clearly underscores the importance of Notch signaling in somitogenesis, but at the same time, it raises the question of why certain genes implicated in somitogenesis on the basis of other evidence did not show up as somite mutants in the Tübingen 1996 screen. In particular, why were no *her*, *fgf* or *wnt* mutations isolated as somite mutants?

A large part of the answer may lie in the usual explanations: the screen did not reach saturation for genes that present a small target for mutagens or that lie in a mutational cold-spot in the genome, and genetic redundancy may mask the effects of mutations that affect only one member of a gene family. These considerations probably account for the failure to find *her1* or *her7* mutations in the original screen. The failure to find *her1* or *her7* mutations may in turn explain why no mutations were found that change the periodicity of the somite clock and thus produce smaller or larger somites, since according to some models the clock periodicity is determined by the properties of these *her* genes (Holley et al., 2002; Lewis, 2003; Oates and Ho, 2002). Moreover, sustained oscillations with an altered period may be difficult to produce by random mutation. Modeling and experimental studies suggest that for the

period-determining clock parameters, there may be only a narrow range within which the clock can continue to function. Thus, an artificial mutation of *Hes7* in the mouse that extends the Hes7 protein half-life from 22 to 30 min leads to a segmentation defect only slightly less severe than in the *Hes7* knockout (Hirata et al., 2004; Lewis, 2003). Complex or extremely specific, and therefore rare, mutations may be needed to produce a noticeable change in the periodicity of the clock without destroying its function, and it may be practically impossible to examine enough mutagenized genomes to isolate such specific mutations in a vertebrate genetic screen.

In the zebrafish, *acerebellar* (*ace*) has been identified as an *fgf8* mutation, but was noticed chiefly for its midbrain–hindbrain boundary defect, although it is also required for normal somitogenesis (Brand et al., 1996; Reifers et al., 1998). The somites in this mutant, however, seem mainly to be reduced in mediolateral and/or dorsoventral dimensions, with relatively little alteration in the anteroposterior positioning of somite boundaries. No *fgf* mutants were found that dramatically alter somite segmentation. One reason may be genetic redundancy between *fgf8* and *fgf24* during tail formation (Draper et al., 2003). A second reason that more severe *fgf* somite mutants were not found may lie in the robustness of the segmentation program: if Fgf activity is genetically reduced throughout segmentation, the system might adjust, for example, by a narrowing of the PSM rather than a change in its anteroposterior extent. In contrast, transient manipulation of Fgf8 signaling may lead to strong transitory morphological effects because such adjustments do not occur instantaneously (Dubrulle et al., 2001; Dubrulle and Pourquié, 2004; Sawada et al., 2001).

Reasons for expecting to find Wnt pathway mutations among the somite segmentation mutants have come from the mouse. *Wnt3a* mutant mice have a segmentation defect in addition to lacking the posterior body, and the Wnt pathway gene *Axin2* has been shown to oscillate in mouse embryos (Aulehla et al., 2003; Takada et al., 1994). Zebrafish Wnt pathway mutants were isolated in the 1996 screens as being required for patterning the neural plate, convergent-extension movements or tail formation, but none affect segmentation of the paraxial mesoderm (Hammerschmidt et al., 1996; Heisenberg et al., 1996, 2000; Jessen et al., 2002; Rauch et al., 1997; Solnica-Krezel et al., 1996; Topczewski et al., 2001). This could be because the *wnt* genes that function during somitogenesis also function in early mesoderm patterning precluding the isolation of somite-specific mutations. Alternatively, Wnt signaling may not play the same role in zebrafish somitogenesis as in the mouse. There is some precedent for such genetic differences between fish and amniotes in the segmentation program, in that *lunatic fringe* and the *delta* genes appear to function differently in mouse, chick and zebrafish somitogenesis (Dale et al., 2003; Prince et al., 2001; Qiu et al., 2004; Sato et al., 2002; Serth et al., 2003) and (reviewed in Giudicelli and Lewis, 2004).

deltaC and deltaD: two Notch ligands, not created equal

Elucidation of the temporal and spatial dynamics of gene expression in the PSM is critical if we wish to understand the mechanisms that regulate somite formation. *her1*, *deltaC* and *her7*, for the most part, oscillate in phase (Gajewski et al., 2003; Holley et al., 2000, 2002; Jiang et al., 2000; Oates and Ho, 2002). However, the middle stripe of *deltaC* precedes the middle stripe of *her1*. This suggests that, at least in this region of the PSM, these oscillating genes are under the control of somewhat different sets of factors. Furthermore, because the *deltaC* stripe precedes the *her1* stripe *only* in the middle of the PSM, the relative importance or mode of action of these regulatory factors must vary from region to region in the PSM.

Our studies of detailed gene expression patterns in *bea/deltaC* and *aei/deltaD* mutants provide some hints as to the basis of the differential gene regulation. The *aei*/*deltaD* and *bea*/*deltaC* mutants differ in several respects. First, while both genes are expressed in a striped pattern in the anterior PSM and in the mature somites, *aei*/*deltaD* does not oscillate in the posterior PSM and is expressed in the anterior half of each somite, whereas *bea*/*deltaC* does oscillate in the posterior PSM and is expressed in the posterior half of each somite (Dornseifer et al., 1997; Holley et al., 2002; Jiang et al., 2000). The differences of expression pattern suggest differences of function, and this suggestion is borne out by the different ways in which *bea* and *aei* mutations affect *deltaC* expression relative to *her1* expression (see Fig. 6). *deltaC* and *deltaD* presumably participate differently in the regulatory feedback loops controlling somitogenesis, which become increasingly complex as additional genes come into play in the anterior PSM.

The *aei*/*deltaD* and *bea*/*deltaC* mutants also differ in the severity of their segmentation defects, which start around the 7th–9th somite in *aei/deltaD* mutants but anywhere from the 2nd–6th somite in *bea/deltaC* mutants (Jiang et al., 2000; van Eeden et al., 1996, 1998). We have found that even the putative null bea^{tit446} homozygotes can display onset of the segmentation defects as late as the 6th somite in some clutches. Thus, while the onset of the somite defect is earlier in *bea*/*deltaC* embryos, it is also more variable and may be sensitive to genetic background. However, within a given clutch, the phenotype is relatively consistent.

Although *bea* homozygotes show a more severe segmentation phenotype than *aei* homozygotes, *aei;bea* doubly homozygous mutants show a segmentation phenotype no more severe than that of the simple *bea* homozygotes: in both cases, the first few somites are spared, and to the same extent. The sparing of these somites in the single homozygotes therefore cannot be simply a result of quasi-redundancy between *deltaC* and *deltaD*, but must have some other explanation. This could lie in the operation of special machinery during formation of these initial somites (Jülich et al., 2005), or could reflect a gradual loss of

synchrony between the oscillations of neighboring cells at the outset of somitogenesis (Jiang et al., 2000), or could be related to occurrence of damped oscillations (Hirata et al., 2004).

Conclusion

In this study, with the cloning of *bea*/*deltaC*, we complete the molecular identification of the somite-segmentation genes identified in the Tübingen 1996 screen. Remarkably, the four genes of this set that are required for operation of the segmentation clock code for components of the Notch pathway, confirming the central role of this signaling pathway in the clock mechanism. The identification of *bea* as *deltaC* has enabled us furthermore to compare and contrast the functions of *aei*/*deltaD* and *bea*/*deltaC* in three developmental processes. In hindbrain neurogenesis, the two *deltas* appear to mediate lateral inhibition in distinct populations of cells. During hypochord formation, *aei*/*deltaD* and *bea*/*deltaC* act in parallel to induce hypochord precursors. But in the segmentation clock, the two genes are both essential and appear to have largely distinct, non-interchangeable functions. Our findings set the stage for future experiments that will be needed to discover the precise, individual roles of *deltaC* and *deltaD* in the segmentation clock machinery.

Acknowledgments

We thank Tim Brend for thoughtful comments on the manuscript. The work on zebrafish somitogenesis and the Notch signaling pathway was supported by a grant from the Agency of Science, Technology and Research (A*STAR), Singapore to Y.-J. J., by Cancer Research UK for A.D. and J.L., and by a grant from the NIH (R01 HD045738-01A1) to S.A.H.

References

Appel, B., Fritz, A., Westerfield, M., Grunwald, D.J., Eisen, J.S., Riley, B.B., 1999. Delta-mediated specification of midline cell fates in zebrafish embryos. Curr. Biol. 9, 247–256.

Artavanis-Tsakonas, S., Rand, M.D., Lake, R.J., 1999. Notch signaling: cell fate control and signal integration in development. Science 284, 770–776.

Aulehla, A., Johnson, R.L., 1999. Dynamic expression of lunatic fringe suggests a link between notch signaling and an autonomous cellular oscillator driving somite segmentation. Dev. Biol. 207, 49–61.

Aulehla, A., Wehrle, C., Brand-Saberi, B., Kemler, R., Gossler, A., Kanzler, B., Herrmann, B.G., 2003. Wnt3a plays a major role in the segmentation clock controling somitogenesis. Dev. Cell 4, 395–406.

Barrios, A., Poole, R.J., Durbin, L., Brennan, C., Holder, N., Wilson, S.W., 2003. Eph/Ephrin signaling regulates the mesenchymal-to-epithelial transition of the paraxial mesoderm during somite morphogenesis. Curr. Biol. 13, 1571–1582.

Bessho, Y., Sakata, R., Komatsu, S., Shiota, K., Yamada, S., Kageyama, R., 2001. Dynamic expression and essential functions of Hes7 in somite segmentation. Genes Dev. 15, 2642–2647.

Bessho, Y., Hirata, H., Masamizu, Y., Kageyama, R., 2003. Periodic repression by the bHLH factor Hes7 is an essential mechanism for the somite segmentation clock. Genes Dev. 17, 1451–1456.

Brand, M., Heisenberg, C.-P., Warga, R., Plegri, F., Karlstrom, R.O., Beuchle, D., Picker, A., Jiang, Y.-J., Furutani-Seiki, M., van Eeden, F.J.M., Granato, M., Haffter, P., Hammerschmidt, M., Kane, D., Kelsh, R., Mullins, M., Odenthal, J., Nüsslein-Volhard, C., 1996. Mutations affecting development of the midline and general body shape during zebrafish embryogenesis. Development 123, 129–142.

Conlon, R.A., Reaume, A.G., Rossant, J., 1995. Notch1 is required for the coordinate segmentation of somites. Development 121, 1533–1545.

Cooke, J., 1998. A gene that resuscitates a theory-somitogenesis and a molecular oscillator. Trends Genet. 14, 85–88.

Cooke, J., Zeeman, E.C., 1975. A clock and wavefront model for control of the number of repeated structures during animal morphogenesis. J. Theor. Biol. 58, 455–476.

Dale, J.K., Maroto, M., Dequeant, M.-L., Malapert, P., McGrew, M., Pourquié, O., 2003. Periodic Notch inhibition by Lunatic Fringe underlies the chick segmentation clock. Nature 421, 275–278.

del Barco Barrantes, I., Elia, A., Wunnch, K., Hrabde De Angelis, M., Mak, T., Rossant, J., Conlon, R., Gossler, A., Luis de la Pompa, J., 1999. Interaction between Notch signaling and Lunatic Fringe during somite boundary formation in the mouse. Curr. Biol. 9, 470–480.

Dornseifer, P., Takke, C., Campos-Ortega, J.A., 1997. Overexpression of a zebrafish homologue of the *Drosophila* neurogenic gene Delta perturbs differentiation of primary neurons and somite development. Mech. Dev. 63, 159–171.

Draper, B.W., Stock, D.W., Kimmel, C.B., 2003. Zebrafish fgf24 functions with fgf8 to promote posterior mesodermal development. Development 130, 4639–4654.

Dubrulle, J., Pourquié, O., 2004. fgf8 mRNA decay establishes a gradient that couples axial elongation to patterning in the vertebrate embryo. Nature 427, 419–422.

Dubrulle, J., McGrew, M.J., Pourquié, O., 2001. FGF signaling controls somite boundary position and regulates segmentation clock control of spatiotemporal hox gene activation. Cell 106, 219–232.

Dunwoodie, S.L., Clements, M., Sparrow, D.B., Sa, X., Conlon, R.A., Beddington, R.S., 2002. Axial skeletal defects caused by mutation in the spondylocostal dysplasia/pudgy gene Dll3 are associated with disruption of the segmentation clock within the presomitic mesoderm. Development 129, 1795–1806.

Durbin, L., Brennan, C., Shiomi, K., Cooke, J., Barrios, A., Shanmugalingam, S., Guthrie, B., Lindberg, R., Holder, N., 1998. Eph signaling is required for segmentation and differentiation of the somites. Genes Dev. 12, 3096–3109.

Durbin, L., Sordino, P., Barrios, A., Gering, M., Thisse, C., Thisse, B., Brennan, C., Green, A., Wilson, S., Holder, N., 2000. Anterior–posterior patterning is required within segments for somite boundary formation in developing zebrafish. Development 127, 1703–1713.

Evrard, Y.A., Lun, Y., Aulehla, A., Gan, L., Johnson, R.L., 1998. Lunatic fringe is an essential mediator of somite segmentation and patterning. Nature 394, 377–381.

Fitzgerald, K., Greenwald, I., 1995. Interchangeability of *Caenorhabditis elegans* DSL proteins and intrinsic signalling activity of their extracellular domains in vivo. Development 121, 4275–4282.

Forsberg, H., Crozet, F., Brown, N.A., 1998. Waves of mouse Lunatic fringe expression, in four-hour cycles at two-hour intervals, precede somite boundary formation. Curr. Biol. 8, 1027–1030.

Gajewski, M., Sieger, D., Alt, B., Leve, C., Hans, S., Wolff, C., Rohr, K.B., Tautz, D., 2003. Anterior and posterior waves of cyclic her1 gene expression are differentially regulated in the presomitic mesoderm of zebrafish. Development 130, 4269–4278.

Geisler, R., Rauch, G.-J., Baier, H., van Bebber, F., Broß, L., Dekens, M., Finger, K., Fricke, C., Gates, M.A., Geiger, H., Geiger-Rudolph, S.,

Gilmour, D., Glaser, S., Gnügge, L., Habeck, H., Hingst, K., Holley, S., Keenan, J., Kirn, A., Knaut, H., Lahkari, D., Maderspacher, F., Martyn, U., Neuhauss, S., Neumann, C., Nicolson, T., Pelegri, F., Ray, R., Rick, J., Roehl, H., Roeser, T., Schauerte, H., Schier, A., Schönberger, U., Schönthaler, H.-B., Schulte-Merker, S., Seydler, C., Talbot, W.S., Weiler, C., Nüsslein-Volhard, C., Haffter, P., 1999. A radiation map of the zebrafish genome. Nat. Genet. 23, 86–89.

Giudicelli, F., Lewis, J., 2004. The vertebrate segmentation clock. Curr. Opin. Genet. Dev. 14, 407–414.

Gray, M., Moens, C.B., Amacher, S.L., Eisen, J.S., Beattie, C.E., 2001. Zebrafish deadly seven functions in neurogenesis. Dev. Biol. 237, 306–323.

Greenwald, I., 1998. LIN-12/Notch signaling: lessons from worms and flies. Genes Dev. 12, 1751–1762.

Haffter, P., Granato, M., Brand, M., Mullins, M.C., Hammerschmidt, M., Kane, D.A., Odenthal, J., van Eeden, F.J.M., Jiang, Y.-J., Heisenberg, C.-P., Kelsh, R.N., Furantani-Seiki, M., Vogelsang, E., Beuchle, D., Schach, U., Fabian, C., Nüsslein-Volhard, C., 1996. The identification of genes with unique and essential functions in the development of the zebrafish, *Danio rerio*. Development 123, 1–36.

Hammerschmidt, M., Nüsslein-Volhard, C., 1993. The expression of a zebrafish gene homologous to *Drosophila* snail suggests a conserved function in invertebrate and vertebrate gastrulation. Development 119, 1107–1118.

Hammerschmidt, M., Pelegri, F., Mullins, M.C., Kane, D.A., Brand, M., van Eeden, F.-J., Furutani-Seiki, M., Granato, M., Haffter, P., Heisenberg, C.-P., Jiang, Y.-J., Kelsh, R.N., Odenthal, J., Warga, R.M., Nüsslein-Volhard, C., 1996. Mutations affecting morphogenesis during gastrulation and tail formation in the zebrafish, *Danio rerio*. Development 123, 143–151.

Heisenberg, C.-P., Brand, M., Jiang, Y.-J., Warga, R.M., Beuchle, D., van Eeden, F.J., Furutani-Seiki, M., Granato, M., Haffter, P., Hammerschmidt, M., Kane, D.A., Kelsh, R.N., Mullins, M.C., Odenthal, J., Nüsslein-Volhard, C., 1996. Genes involved in forebrain development in the zebrafish, *Danio rerio*. Development 123, 191–203.

Heisenberg, C.P., Tada, M., Rauch, G.J., Saude, L., Concha, M.L., Geisler, R., Stemple, D.L., Smith, J.C., Wilson, S.W., 2000. Silberblick/Wnt11 mediates convergent extension movements during zebrafish gastrulation. Nature 405, 76–81.

Henderson, S.T., Gao, D., Christensen, S., Kimble, J., 1997. Functional domains of LAG-2, a putative signaling ligand for LIN-12 and GLP-1 receptors in *Caenorhabditis elegans*. Mol. Biol. Cell 8, 1751–1762.

Henry, C.A., Hall, L.A., Hille, M.B., Solnica-Krezel, L., Cooper, M.S., 2000. Somite in zebrafish doubly mutant for knypek and trilobite form without internal mesenchymal cells or compaction. Curr. Biol. 10, 1063–1066.

Henry, C.A., Urban, M.K., Dill, K.K., Merlie, J.P., Page, M.F., Kimmel, C.B., Amacher, S.L., 2002. Two linked hairy/enhancer of split-related zebrafish genes, her1 and her7, function together to refine alternating somite boundaries. Development 129, 3693–3704.

Hirata, H., Bessho, Y., Kokubu, H., Masamizu, Y., Yamada, S., Lewis, J., Kageyama, R., 2004. Instability of Hes7 protein is crucial for the somite segmentation clock. Nat. Genet. 36, 750–754.

Holley, S.A., Takeda, H., 2002. Catching a wave: the oscillator and wavefront that create the zebrafish somite. Semin. Cell Dev. Biol. 13, 481–488.

Holley, S.A., Geisler, R., Nüsslein-Volhard, C., 2000. Control of her1 expression during zebrafish somitogenesis by a Delta-dependent oscillator and an independent wave-front activity. Genes Dev. 14, 1678–1690.

Holley, S.A., Jülich, D., Rauch, G.J., Geisler, R., Nüsslein-Volhard, C., 2002. her1 and the notch pathway function within the oscillator mechanism that regulates zebrafish somitogenesis. Development 129, 1175–1183.

Hrabé Angelis, M., McIntyre, J., Gossler, A., 1997. Maintenance of somite borders in mice requires the Delta homologue Dll1. Nature 386, 717–721.

Itoh, M., Kim, C.H., Palardy, G., Oda, T., Jiang, Y.-J., Maust, D., Yeo, S.Y., Lorick, K., Wright, G.J., Ariza-McNaughton, L., Weissman, A.M., Lewis, J., Chandrasekharappa, S.C., Chitnis, A.B., 2003. Mind bomb is a ubiquitin ligase that is essential for efficient activation of Notch signaling by Delta. Dev. Cell 4, 67–82.

Jen, W.-C., Wettstein, D., Turner, D., Chitnis, A., Kintner, C., 1997. The Notch ligand, X-Delta-2, mediates segmentation of the paraxial mesoderm in *Xenopus* embryos. Development 124, 1169–1178.

Jen, W.C., Gawantka, V., Pollet, N., Niehrs, C., Kintner, C., 1999. Periodic repression of Notch pathway genes governs the segmentation of *Xenopus* embryos. Genes Dev. 13, 1486–1499.

Jessen, J.R., Topczewski, J., Bingham, S., Sepich, D.S., Marlow, F., Chandrasekhar, A., Solnica-Krezel, L., 2002. Zebrafish trilobite identifies new roles for Strabismus in gastrulation and neuronal movements. Nat. Cell Biol. 4, 610–615.

Jiang, Y.-J., Brand, M., Heisenberg, C.-P., Beuchle, D., Furutani-Seiki, M., Kelsh, R.N., Warga, R.M., Granato, M., Haffter, P., Hammerschmidt, M., Kane, D.A., Mullins, M.C., Odenthal, J., van Eeden, F.J.M., Nüsslein-Volhard, C., 1996. Mutations affecting neurogenesis and brain morphology in the zebrafish, *Danio rerio*. Development 123, 205–216.

Jiang, Y.-J., Aerne, B.L., Smithers, L., Haddon, C., Ish-Horowicz, D., Lewis, J., 2000. Notch signaling and the synchronization of the somite segmentation clock. Nature 408, 475–479.

Jouve, C., Palmeirim, I., Henrique, D., Beckers, J., Gossler, A., Ish Horowicz, D., Pourquié, O., 2000. Notch signalling is required for cyclic expression of the hairy-like gene HES1 in the presomitic mesoderm. Development 127, 1421–1429.

Jowett, T., 2001. Double in situ hybridization techniques in zebrafish. Methods 23, 345–358.

Jülich, D., Geisler, R., Consortium, T.S., Holley, S.A., 2005. Integrina5 and Delta/Notch signalling have complementary spatiotemporal requirements during zebrafish somitogenesis. Dev. Cell, 575–586.

Kim, C.H., Ueshima, E., Muraoka, O., Tanaka, H., Yeo, S.Y., Huh, T.L., Miki, N., 1996. Zebrafish elav/HuC homologue as a very early neuronal marker. Neurosci. Lett. 216, 109–112.

Kim, S.H., Jen, W.C., De Robertis, E.M., Kintner, C., 2000. The protocadherin PAPC establishes segmental boundaries during somitogenesis in *Xenopus* embryos. Curr. Biol. 10, 821–830.

Kimmel, C.B., Ballard, W.M., Kimmel, S.R., Ullmann, B., Schilling, T.F., 1995. Stages of embryonic development of the zebrafish. Dev. Dynam. 203, 253–310.

Koshida, S., Kishimoto, Y., Ustumi, H., Shimizu, T., Furutani-Seiki, M., Kondoh, H., Takada, S., 2005. Integrinalpha5-dependent fibronectin accumulation for maintenance of somite boundaries in zebrafish embryos. Dev. Cell 8, 587–598.

Kulesa, P., Fraser, S.E., 2002. Cell dynamics during somite boundary formation revealed by time-lapse analysis. Science 298, 991–995.

Kusumi, K., Sun, E.S., Kerrebrock, A.W., Bronson, R.T., Chi, D.C., Bulotsky, M.S., Spencer, J.B., Birren, B.W., Frankel, W.N., Lander, E.S., 1998. The mouse pudgy mutation disrupts Delta homologue Dll3 and initiation of early somite boundaries. Nat. Genet. 19, 274–278.

Latimer, A.J., Dong, X., Markov, Y., Appel, B., 2002. Delta–Notch signaling induces hypochord development in zebrafish. Development 129, 2555–2563.

Leimeister, C., Dale, K., Fischer, A., Klamt, B., Hrabe de Angelis, M., Radtke, F., McGrew, M.J., Pourquié, O., Gessler, M., 2000. Oscillating expression of c-Hey2 in the presomitic mesoderm suggests that the segmentation clock may use combinatorial signaling through multiple interacting bHLH factors. Dev. Biol. 227, 91–103.

Lewis, J., 2003. Autoinhibition with transcriptional delay: a simple mechanism for the zebrafish somitogenesis oscillator. Curr. Biol. 13, 1398–1408.

McGrew, M.J., Dale, J.K., Fraboulet, S., Pourquié, O., 1998. The Lunatic Fringe gene is a target of the molecular clock linked to segmentation in avian embryos. Curr. Biol. 8, 979–982.

Meinhardt, H., 1982. Models of Biological Pattern Formation. Academic Press.

Meinhardt, H., 1986. Models of segmentation. In: Bellairs, R., Ede, D.A., Lash, J.W. (Eds.), Somites in Developing Embryos, vol. 18. Plenum Press, pp. 178–189.

Nakaya, Y., Kuroda, S., Katagiri, Y.T., Kaibuchi, K., Takahashi, Y., 2004. Mesenchymal–epithelial transition during somitic segmentation is regulated by differential roles of Cdc42 and Rac1. Dev. Cell 7, 425–438.

Nikaido, M., Kawakami, A., Sawada, A., Furutani-Seiki, M., Takeda, H., Araki, K., 2002. Tbx24, encoding a T-box protein, is mutated in the zebrafish somite-segmentation mutant fused somites. Nat. Genet. 31, 195–199.

Nüsslein-Volhard, C., Dahm, R., 2002. Zebrafish. In: Hames, B.D. (Ed.), Practical Approach. Oxford Univ. Press, Oxford, UK, p. 303.

Oates, A.C., Ho, R.K., 2002. Hairy/E(spl)-related (Her) genes are central components of the segmentation oscillator and display redundancy with the Delta/Notch signaling pathway in the formation of anterior segmental boundaries in the zebrafish. Development 129, 2929–2946.

Oates, A.C., Mueller, C., Ho, R.K., 2005. Cooperative function of deltaC and her7 in anterior segment formation. Dev. Biol. 280, 133–149.

Oka, C., Nakano, T., Wakeham, A., de la Pompa, J.L., Mori, C., Sakai, T., Okazaki, S., Kawaichi, M., Shiota, K., Mak, T.W., Honjo, T., 1995. Disruption of the mouse RBP-J Kappa results in early embryonic death. Development 121, 3291–3301.

Oxtoby, E., Jowett, T., 1993. Cloning of the zebrafish krox-20 gene (krx-20) and its expression during hindbrain development. Nucleic Acids Res. 21, 1087–1095.

Palmeirim, I., Henrique, D., Ish-Horowicz, D., Pourquié, O., 1997. Avian hairy gene expression identifies a molecular clock linked to vertebrate segmentation and somitogenesis. Cell 91, 639–648.

Parks, A.L., Klueg, K.M., Stout, J.R., Muskavitch, M.A., 2000. Ligand endocytosis drives receptor dissociation and activation in the Notch pathway. Development 127, 1373–1385.

Pourquié, O., 2003. The segmentation clock: converting embryonic time into spatial pattern. Science 301, 328–3230.

Prince, V.E., Holley, S.A., Bally-Cuif, L., Prabhakaran, B., Oates, A.C., Ho, R.K., Vogt, T.F., 2001. Zebrafish lunatic fringe demarcates segmental boundaries. Mech. Dev. 105, 175–180.

Qiu, X., Xu, H., Haddon, C., Lewis, J., Jiang, Y.J., 2004. Sequence and embryonic expression of three zebrafish fringe genes: lunatic fringe, radical fringe, and manic fringe. Dev. Dyn. 231, 621–630.

Rauch, G.J., Hammerschmidt, M., Blader, P., Schauerte, H.E., Strahle, U., Ingham, P.W., McMahon, A.P., Haffter, P., 1997. Wnt5 is required for tail formation in the zebrafish embryo. Cold Spring Harbor Symp. Quant. Biol. 62, 227–234.

Reifers, F., Bohli, H., Walsh, E.C., Crossley, P.H., Stainier, D.Y., Brand, M., 1998. Fgf8 is mutated in zebrafish acerebellar (ace) mutants and is required for maintenance of midbrain–hindbrain boundary development and somitogenesis. Development 125, 2381–2395.

Rida, P.C., Le Minh, N., Jiang, Y.-J., 2004. A Notch feeling of somite segmentation and beyond. Dev. Biol. 265, 2–22.

Saga, Y., Hata, N., Koseki, H., Taketo, M.M., 1997. Mesp2: a novel mouse gene expressed in the presegmented mesoderm and essential for segmentation initiation. Genes Dev. 11, 1827–1839.

Sato, Y., Yasuda, K., Takahashi, Y., 2002. Morphological boundary forms by a novel inductive event mediated by Lunatic fringe and Notch during somitic segmentation. Development 129, 3633–3644.

Sawada, A., Fritz, A., Jiang, Y.-J., Yamamoto, A., Yamasu, K., Kuroiwa, A., Saga, Y., Takeda, H., 2000. Zebrafish Mesp family genes, mesp a and mesp b are segmentally expressed in the presomitic mesoderm, Mesp b confers the anterior identity to the developing somites. Development 127, 1691–1702.

Sawada, A., Shinya, M., Jiang, Y.-J., Kawakami, A., Kuroiwa, A., Takeda, H., 2001. Fgf/MAPK signalling is a crucial positional cue in somite boundary formation. Development 128, 4873–4880.

Serth, K., Schuster-Gossler, K., Cordes, R., Gossler, A., 2003. Transcriptional oscillation of lunatic fringe is essential for somitogenesis. Genes Dev. 17, 912–925.

Smithers, L., Haddon, C., Jiang, Y.-J., Lewis, J., 2000. Sequence and embryonic expression of deltaC in the zebrafish. Mech. Dev. 90, 119–123.

Solnica-Krezel, L., Stemple, D.L., Mountcastle-Shah, E., Rangini, Z., Neuhauss, S.C., Malicki, J., Schier, A.F., Stainier, D.Y., Zwartkruis, F., Abdelilah, S., Driever, W., 1996. Mutations affecting cell fates and cellular rearrangements during gastrulation in zebrafish. Development 123, 67–80.

Takada, S., Stark, K.L., Shea, M.J., Vassileva, G., McMahon, J.A., McMahon, A.P., 1994. Wnt-3a regulates somite and tailbud formation in the mouse embryo. Genes Dev. 8, 174–189.

Takahashi, Y., Koizumi, K., Takagi, A., Kitajima, S., Inoue, T., Koseki, H., Saga, Y., 2000. Mesp2 initiates somite segmentation through the Notch signalling pathway. Nat. Genet. 25, 390–396.

Takke, C., Campos-Ortega, J.A., 1999. her1, a zebrafish pair-rule gene, acts downstream of notch signaling to control somite development. Development 126, 3005–3014.

Topczewska, J.M.J.T., Shostak, A., Kume, T., Solnica-Krezel, L., Hogan, B.L., 2001. The winged helix transcription factor Foxc1a is essential for somitogenesis in zebrafish. Genes Dev. 15, 2483–2493.

Topczewski, J., Sepich, D.S., Myers, D.C., Walker, C., Amores, A., Lele, Z., Hammerschmidt, M., Postlethwait, J., Solnica-Krezel, L., 2001. The zebrafish glypican knypek controls cell polarity during gastrulation movements of convergent extension. Dev. Cell 1, 251–264.

van Eeden, F.J.M., Granato, M., Schach, U., Brand, M., Furutani-Seiki, M., Haffter, P., Hammerschmidt, M., Heisenberg, C.-P., Jiang, Y.-J., Kane, D.A., Kelsh, R.N., Mullins, M.C., Odenthal, J., Warga, R.M., Allende, M.L., Weinberg, E.S., Nüsslein-Volhard, C., 1996. Mutations affecting somite formation and patterning in the zebrafish *Danio rerio*. Development 123, 153–164.

van Eeden, F.J.M., Holley, S.A., Haffter, P., Nüsslein-Volhard, C., 1998. Zebrafish segmentation and pair-rule patterning. Dev. Genet. 23, 65–76.

Weinmaster, G., Kintner, C., 2003. Modulation of Notch signaling during somitogenesis. Annu. Rev. Cell Dev. Biol. 19, 367–395.

Wong, P.C., Zheng, H., Chen, H., Becher, M.W., Sirinathsinghji, D.J.S., Trumbauer, M.E., Chen, H.Y., Price, D.L., Van der Ploeg, L.H.T., Sisodia, S.S., 1997. Presenilin 1 is required for Notch1 and Dll1 expression in the paraxial mesoderm. Nature 387, 288–292.

Yan, Y.L., Hatta, K., Riggleman, B., Postlethwait, J.H., 1995. Expression of a type II collagen gene in the zebrafish embryonic axis. Dev. Dyn. 203, 363–376.

Zhang, N., Gridley, T., 1998. Defects in somite formation in lunatic fringe deficient mice. Nature 394, 374–377.